Truncation mutagenesis of Porcine Circovirus 1 VP3 uncovers the importance of the C-terminal extended region in inducing apoptosis of human cancer cells

A Major Qualifying Project

submitted to the faculty of

WORCESTER POLYTECHNIC INSTITUTE

in partial fulfillment of the requirements for the

Degree of Bachelor of Science in Biochemistry

by

Evgenia J. Filatava

and

Phuong T. Vu

April 30, 2015

Approved by

Dr. Destin Heilman, Advisor

Department of Chemistry and Biochemistry, WPI

ABSTRACT

The third viral protein (VP3) of Chicken Anemia Virus (CAV) has been shown to induce apoptosis in cancer cells, while leaving normal cells intact. A homolog of CAV VP3, Porcine Circovirus Type 1 (PCV1) VP3, is also known to be cytotoxic to cancer cells. Sequence analysis has shown that PCV1 VP3 contains an N-terminal region homologous to CAV VP3 and a C-terminal extended region. To identify the region of PCV1 VP3 responsible for its apoptotic activity, transfection of H1299 cell line followed by apoptosis studies were conducted with truncated and chimeric constructs. The apoptotic responses induced by the full length or the C-terminal extended region of PCV1 VP3 were significantly higher than those induced by the control vector. In contrast, the N-terminal homologous region of PCV1 VP3 had unremarkable apoptosis levels, similar to the control vector. These results suggest that the C-terminal extended region of PCV1 VP3 is necessary for inducing apoptosis in cancer cells.

ACKNOWLEDGEMENTS

First and foremost, we would like to thank Professor Destin Heilman for his exceptional support as our advisor, for his patient guidance throughout the project, and for numerous stimulating discussions in the course of this work. We would also like to acknowledge Edward Partlow for his collaboration in preparation of necessary experimental materials. We appreciate the efforts of Kenneth Hough and Andrew Rogers whose contributions to the study of PCV1 VP3 provided the basis of our research. Finally, we would like to thank Professor Rick Wobbe for providing valuable laboratory advice.

TABLE OF CONTENTS

TABLE OF FIGURES

INTRODUCTION

Cancer is the second leading cause of death in the United States, accounting for nearly 1 of every 4 deaths. Nation's leading cancer organizations estimate over 1.5 million of new cancer cases and 0.5 million cancer deaths in 2014 [3]. While there are more than 100 distinct types of cancer, all of them begin in cells that fail to follow the normal cell cycle and instead divide uncontrollably [7]. Over time, cancer cells diverge even further from normalcy and continue to proliferate with damaged DNA, which leads to new mutations. As a result of accumulating mutations, cancer cells become increasingly resistant to the signals that maintain normal tissue. Notably, cancer cells exhibit accelerated cell division rates and have impaired controls responsible for DNA damage repair, cell cycle arrest, and programmed cell death that would normally render them prime targets for apoptosis [15].

While different cancers have different mutational signatures, one of the most common mutations involves inactivation of the genes that suppress cell proliferation or those that signal the need for apoptosis. These genes, known as tumor suppressor genes, play an essential role in surveillance of DNA damage, regulating cell division, and preventing tumor formation. Many cancer cells carry two mutated copies of the *TP53* tumor suppressor gene that codes for p53, a multifunctional protein that normally senses cellular and genetic damage [15]. The expression of this tumor suppressor protein can be triggered by a number of physical or chemical DNA-damaging agents such as gamma irradiation, UV rays, oxidizing agents, cytotoxic drugs, and cancer-causing chemicals. Once activated, p53 normally regulates checkpoint genes and proteins involved in cell cycle arrest (in G1, G1/S, and G2/M) in replication, transcription, DNA repair, and apoptosis [5]. However, even small mutations in *TP53* can lead to a nonfunctional version of p53 and result in carcinogenesis [15].

Inactivation of p53 function due to mutations in *TP53* gene is an almost universal feature of cancer cells and thus, a major hurdle in the development of anti-cancer therapies [20]. Current mainstream non-surgical treatment options, including chemotherapy, radiation, and immunotherapy, are known for their often low success rates and negative side effects [20]. Poor response to current therapies is largely attributed to their reliance on functional p53 to induce apoptosis, and their undesired side effects arise from the damage they cause to surrounding healthy cells. Therefore, development of effective cancer therapies hinges on the discovery of agents that can selectively destroy cancer cells while leaving normal cells intact. Furthermore, studying alternative mechanisms of inducing apoptosis in cancer cells that do not rely on a p53-dependent pathway may open up new avenues for effective treatments that can target a variety of cancers [9].

Apoptosis is a fundamental physiological form of cell death that mediates the elimination of cancerous or virus-infected cells. Regulation of caspase activation is one of the key events in apoptosis. All apoptotic caspases exist in normal cells as inactive enzymes known as procaspases. When cells undergo apoptosis, these procaspases are sequentially activated through proteolytic processing at aspartic acid residues that cleaves the single peptide precursor into the large and small fragments that constitute the active enzyme [22].

There are currently two main caspase-activating cascades that regulate apoptosis. The first, referred to as the extrinsic or cytoplasmic pathway, requires the binding of ligands to their corresponding death receptors (e.g. TNFR superfamily) on the plasma membrane, which results in the assembly of adaptor molecules and caspase-8 activation. The second pathway is the intrinsic or mitochondrial pathway in which the activation of the Bcl-2 family of proteins causes the release of cytochrome-c from the mitochondria, which then facilitates the formation of the

apoptosome and caspase-9 activation. Both pathways involving active initiator caspases converge to a final common pathway involving the activation of a cascade of executioner caspases, such as the caspases-3 and -7, culminating in the death of targeted cells. This cascade of events ensures the quick generation of a massive amount of active caspases capable of cleaving a wide range of cellular proteins in order to dismantle cells. Caspases also affect cytoskeletal structure, cell cycle regulation, and signaling pathways, ultimately leading to the morphologic manifestations of apoptosis, such as cell shrinkage, plasma and nuclear membrane blebbing, DNA condensation and fragmentation, and production of membrane-enclosed particles containing intracellular material known as apoptotic bodies [22].

Since the activation of apoptosis by the extracellular death receptors requires external stimuli, this pathway renders many challenges for the design of cancer-specific therapeutical agents. The intrinsic pathway, however, involves activation of apoptosis from within the cell and therefore, is a more suitable choice for the mechanism of novel cancer treatments. The ability to intrinsically induce apoptosis is known to be harbored by some naturally-existing proteins. For example, several animal viruses have evolved proteins that target vulnerable checkpoints responsible for activation of apoptosis inside their host cells in order to facilitate their own replication [8]. By modulating key cell cycle regulators, these viruses are able to first inhibit apoptosis to maximize viral replication and then, to induce apoptosis near the end of their life cycle to promote viral spreading outside of their host cell [18]. In certain cases, these viruses select for cells that would promote maximum viral propagation, thereby making their apoptotic activity exclusive to cancer cells [8]. One example of a well-characterized proapoptotic virus is the chicken anemia virus (CAV), which encodes a cancer selective third viral protein (VP3).

CAV − the sole member of the family *Circoviridae*, genus *Gyroviridae* − is responsible for causing severe anemia in young chickens by replicating and inducing large-scale apoptosis of cortical thymocytes and erythroblasts in the bone marrow [11]. CAV is a non-enveloped, circular, single-stranded DNA virus with a small genome of 2.3 kb which contains two major open reading frames (ORFs) [24]. ORF1 encodes for viral replication proteins, while ORF2 encodes for the immunogenic capsid protein. The third viral protein (VP3) encoded by ORF3 has shown to be a potent inducer of apoptosis in a variety of human cancer cell line [25]. Importantly, it has been shown to possess both nuclear import and export signals. These signal sequences have been linked to the ability of this protein to engage in cell-type specific apoptosis. Specifically, the apoptotic activity of CAV VP3 is thought to be regulated by nuclear localization since it is found in the nucleus of transformed cells and in the cytoplasm of primary cells [10]. It has been further shown that CAV VP3 interacts with subunit 1 of the anaphase-promoting complex/cyclosome (APC/C), a major regulator of the cell cycle, which results in G2/M cell cycle arrest and subsequent induction of apoptosis [16, 21]. Two properties of CAV VP3-induced apoptosis make it of a significant therapeutic interest. First, CAV VP3 only induces apoptosis in cancer cells while leaving normal cells intact [1]. Second, the induction of apoptosis in cancer cells occurs regardless of the status of the p53 tumor suppressor [2]. Therefore, CAV VP3 represents a novel, selective agent for the treatment of tumors that are resistant to many of current cancer therapies as a result of nonfunctional p53.

Another virus similar to CAV that shares approximately 55% sequence homology and has shown promise in cancer research is Porcine circovirus (PCV) [17]. Originating from the same *Circoviridae* family, PCV is a non-enveloped, circular, single-stranded DNA virus with a 1.76 kb genome and two main serotypes, type 1 and type 2 [14]. Porcine circovirus type 1

(PCV1) was initially discovered in 1974 by Tischer et al. as a picornavirus-like contaminant of the pig kidney cell line PK/15 [23]. PCV1 was later characterized as a readily infectious, but a non-pathogenic virus. Unlike PCV1, porcine circovirus type 2 (PCV2), first recognized in 1991, is associated with a number of disease syndromes such as postweaning multisystemic wasting syndrome (PMWS), a disease causing immunosuppression in pigs [19]. Although PCV1 and PCV2 differ in virulence, their genomes have shown to be similar with approximately 78% nucleotide homology [6]. Similar to CAV, both viral genomes of PCV1 and PCV2 have two major open reading frames, ORF1 and ORF2, and also contain an ORF3, which encodes the VP3. While PCV2 is divided into two serotypes with distinctive pathophysiology [4], PCV2a and PCV2b, both produce a protein from ORF3 that has reported apoptotic capacity similar to CAV VP3 [12, 13]

Until recently, very little was known about PCV1, a non-pathogenic cousin of PCV2 and CAV. Hough et al. hypothesized that PCV1 also harbors a third ORF, which may produce a protein with similar functional capacities [10]. Their study revealed ORF3 on the PCV1 genome consisting of 207 aa and its comparison with translated ORF3 of PCV2a/b resulted in 62% sequence identity. Interestingly, they reported a high degree of homology in the N-terminal region among nt 1–312 (aa 1-104). However, a nucleotide alignment revealed a difference at nt 315 resulting in a tyrosine codon in PCV1 where a stop codon exists in both of PCV2 serotypes. After nt 315, the PCV1 ORF3 sequence codes for a highly hydrophobic C-terminal region (aa 105–207), which nearly doubles the size of the gene compared with homologous sequences of PCV2a/b ORF3. Sequence alignment of PCV1 VP3 with CAV VP3 also revealed clustered sections of homologous residues concentrated around the nuclear export and import sequences of CAV VP3, which have been shown to be critical for its apoptotic function.

Demonstrated sequence homology and functional similarity between apoptotic CAV VP3, PCV2a/b VP3, and poorly characterized PCV1 VP3 call for further investigation of PCV1 VP3. The goal of this study is to quantitatively determine the apoptotic ability of wt PCV1 VP3 in cancer cells. Furthermore, since sequence analysis of PCV1 VP3 revealed an N-terminal region homologous to CAV VP3 and a C-terminal extended region, we are interested in determining which of these two regions is responsible for apoptotic activity of PCV1 VP3. We aim to investigate the role of each region of PCV1 VP3 through the use of wild-type constructs, as well as truncated and chimeric mutants. By comparing apoptotic capability of the aforementioned constructs, we shall be able to analyze the significance of each region of PCV1 VP3 in terms of its contribution to apoptosis induction.

MATERIALS AND METHODS

Cell Culture Maintenance

Human non-small cell lung carcinoma H1299 cell line (p53-null) was maintained in Dulbecco's modified Eagle medium supplemented with 10% fetal bovine serum. Cells were incubated at 37°C in 5% CO_2 : 95% air and passaged regularly using 0.05% trypsin before reaching 80-90% confluence.

Transient Transfection

H1299 cells used for G418 antibiotic selection were transiently transfected with six previously made pEGFP-C1 constructs under the control of a constitutive cytomegalovirus (CMV) promoter using Effectene Transfection Reagent kit (Qiagen). Wild-type CAV VP3 (EGFP – wt CAV VP3) and wild-type PCV1 VP3 (EGFP – wt PCV1 VP3) were used as positive apoptosis controls, while an empty EGFP vector and a no transfection sample were used as negative apoptosis controls. Cells were passaged at 40-50% confluence into 6-well plates and transfected after a day of incubation when the cell confluence had reached 80-90%. The amount of construct DNA used (ranging from 0.7-1.4 μg/well) was optimized to achieve approximately 60% of protein expression across all samples, while the rest of the manufacturer's protocol was executed without modifications.

Fluorescence Microscopy and Antibiotic Selection

Two days post-transfection, the percent of cells expressing viral proteins (regardless of the intensity) were detected by visualizing the presence and distribution of EGFP expression using fluorescence microscopy and imaged with a Zeiss Vert.A1 fluorescence microscope using SPOT 5.1 Basic software. The EGFP expression was then quantified using ImageJ (National

Institute of Health) based on pixel intensity by normalizing the images to the no transfection sample and converting them to a greyscale to improve contrast.

The cells were then treated with G418 [800 μg/ml] for EGFP-tagged gene selection. After 2 days of selection, G418-containing medium was replaced with an increased concentration of G418 [1200 μg/ml]. The selected cells were then prepared for the viability assay in the next two days.

Viability Assay

After 4 days of G418 selection, H1299 cells were washed in 1% PBS, fixed for 15 min with 4% paraformaldehyde prepared in 1% PBS, washed two more times in 1% PBS, and stained for 20 min with 0.1% (w/v) crystal violet prepared in 10% ethanol. Following staining, cells were washed with water to remove excess dye and photographed for a visual assessment of cell viability. The dye taken up by the cells was then solubilized with 2% (w/v) sodium dodecyl sulfate (SDS) and the plates were allowed to rock for 1 hour. The optical density (OD) was measured at 590 nm using a Genesys 20 Visible Spectrophotometer (Thermo Scientific). The OD values were converted into the cell viability % by the formula, cell viability % = (OD value of experimental group / OD value of control group) × 100%.

EXPERIMENTAL PROTOCOL

The protocol below describes all experiments used in this study to ultimately assess the apoptotic activity of EGFP-tagged constructs in p53-null non-small cell lung carcinoma H1299 cell line.

Cell culture maintenance

H1299 cells were maintained in a T25 culture flask (25cm^2) in Dulbecco's modified Eagle medium supplemented with 10% fetal bovine serum. Cells were incubated at 37°C in 5% CO_2 : 95% air and passaged regularly using 0.05% trypsin before reaching 80-90% confluence.

Day 0: Passage of H1299 cells into 6-well-plates

1. Aspirate off the media in the T25 flask and wash the cells with 5 ml of 1% phosphate-buffered saline (PBS).
2. Coat the cells with 0.5 ml of 0.05% trypsin and aspirate immediately after ~20 seconds.
3. Once the cells have detached from the flask, resuspend them in 5 ml of media to neutralize trypsin.
4. Plate an appropriate amount of cell suspension into a well of the 6-well plate (9.61cm^2/well) to achieve 40-50% confluence in each well. Add enough media to bring the total volume in each well to 2 ml. Note: depending on the number of samples that need to be tested, the amount of cells needed prior to passage may vary.
5. Incubate the cells under their optimal growth conditions. The well should be approximately 80-90% confluent on the day of transfection.

Day 1: Transient transfection

H1299 cells were transiently transfected with viral constructs using Effectene Transfection Reagent kit (Qiagen). The amount of construct DNA (μg) used was optimized to achieve approximately 60% protein expression across all samples (see Table 1), while the rest of the manufacturer's protocol was executed without modifications.

Table 1: Optimal amount of plasmid DNA for transient transfection of H1299 cells.

EGFP-tagged constructs	DNA (μg)
wt CAV VP3 (1-121)	0.7
wt PCV1 VP3 (1-207)	1.4
PCV1 VP3 (1-105)	0.9
PCV1 VP3 (105-207)	1.3
CAV VP3 (1-121) – PCV1 VP3 (105-207)	1.2
EGFP	0.8

Day 3: Assessment of EGFP expression

Two days post-transfection, the percentage of cells expressing viral proteins (regardless of the intensity) were detected by visualizing the presence and distribution of EGFP expression using fluorescence microscopy and imaged with a Zeiss Vert.A1 fluorescence microscope using SPOT 5.1 Basic software. The EGFP expression was then quantified using ImageJ (National Institute of Health) by normalizing the images of tested constructs to the no transfection sample and converting them to a grayscale. Note that the EGFP expression of transfected H1299 cells in each panel was quantified by measuring white pixel intensity. However, since the intensity of EGFP varies among the constructs, the data quantified by ImageJ did not recapitulate our visual assessment of the percentage of cells expressing viral proteins. Alternatively, to achieve a more accurate measurement, flow cytometry may be used to quantify the amount of construct-positive cells since the apoptotic activity of the constructs was observed only two days post-transfection.

Day 3 - 7: Geneticin selection

Following confirmation of protein expression, the cells were then treated with Geneticin (G418) and selected for EGFP-positive cells for 4 days or until all of the cells in the no transfection sample treated with G418 were removed.

Day 3

1. Prepare G418 medium at 800 μg/ml (note: you may choose to use the same concentration of G418 mediumas used on Day 5 [1200 μg/ml] throughout the selection period for future experiments).
2. Aspirate off the old G418-free media and wash the cells with 2 ml of 1% PBS.
3. Coat the cells in each well with 0.2 ml of 0.05% trypsin and aspirate immediately after ~20 seconds.
4. Once the cells have detached from the well, resuspend them using a P1000 micropipette in 2 ml of G418 media to neutralize trypsin.
5. In a new 6-well-plate, split the cell suspension at 7:10 ratio and add enough G418 media to bring the total volume to 2 ml.

Day 5

1. Prepare G418 medium at 1200 μg/ml and follow the steps above to continue G418 selection.

Day 7: Crystal violet staining and assessment of viability

After 4 days of G418 selection, H1299 cells were stained with crystal violet for visualization of the remaining viable cells. To minimize cell detachment, make sure to pipette all

of the solutions very gently by dispensing them down the wall of the well while rotating the plate.

1. Aspirate off the old G418 media and wash the cells twice with 1 ml of 1% PBS.
2. Fix for 15 minutes with 1 ml of 4% paraformaldehyde prepared in 1% PBS.
3. Wash the cells two more times with 1 ml of 1% PBS.
4. Add 0.75 ml of 0.1% (w/v) crystal violet prepared in 10% ethanol and stain the cells for 20 minutes.
5. Following staining, wash the cells with distilled water until it runs clear to remove excess dye.
6. Let the plates dry overnight and image the wells for a visual assessment of cell viability.
7. Solubilize the dye taken up by the cells with 2% (w/v) sodium dodecyl sulfate (SDS) and rock the plate for 1 hour.
8. Measure the optical density (OD) of the solubilized stain at 590 nm using a Genesys 20 Visible Spectrophotometer (Thermo Scientific). Dilute the sample if necessary since the concentration of the solubilized stain may be too high for the spectrophotometer to detect. The OD values were converted into the cell viability % by the following formula:
   cell viability % = (OD value of experimental group / OD value of control group) × 100%.

RESULTS

The ability of Chicken Anemia Virus third viral protein (CAV VP3) and Porcine Circovirus Type 1 third viral protein (PCV1 VP3) to induce apoptosis in human cancer cells without a functional p53 protein makes them potential candidates for the development of new cancer therapies. While CAV VP3 has been well-characterized, very little is known about PCV1 VP3. We are interested in understanding how efficiently PCV1 VP3 induces apoptosis as well as identifying the region of the protein responsible for its apoptotic activity.

Previously, several mutants of PCV1 VP3 were created to study its apoptosis-inducing property. However, the constructs have not been characterized because all previous attempts using fluorescence-based assays have failed to clearly detect apoptotic activity in cancer cells. These assays are based on a reagent called fluorescence-labeled inhibitor of caspases. The reagent enters each cell and irreversibly binds to activated caspases with a preference for its target peptide sequence. Analysis of cells containing bound reagents by fluorescence microscopy then gives a direct measure of apoptosis induced by each construct. These caspase detection assays seemed promising at the beginning but proved to be an unsuitable choice due to various reasons. Specifically, the substantial rate of apoptosis in cancer cells, due to their rapid proliferation, results in an excessive level of apoptosis background noise in construct-negative cells. Additionally, the process of transfecting DNA into cells is toxic to some extent and thus, further contributes to the high level of apoptosis background. At the same time, the fluorescence signal from the caspase inhibitor was relatively weak, making it challenging to clearly detect the apoptotic activity in cancer cells. Furthermore, the lipid-based transfection assay used in this study does not yield as high transfection efficiency as, for example, adenovirus transduction (almost 100%). Thus, only a subpopulation of cancer cells contains the constructs and expresses

the proteins of interest. Besides, the fluorescence-based apoptosis detection kit used in this study was specific for the caspase-3 and -7 pathway. Since the caspases involved in the apoptosis of our target constructs have yet to be identified, the kit may not detect the appropriate caspase activity. Taking all of these reasons into account, there was a need for a method that can potentially remove all construct-negative cells to reduce the background noise, detect apoptosis regardless of the exact caspase pathways involved, and produce readily interpretable data.

After examining several strategies, we took advantage of the antibiotic resistance gene (neomycin/kanamycin) in the EGFP-C1 vector used for cloning to select for construct-positive cells and then, determined their apoptotic activity using crystal violet staining. To that end, it took a lot of refinement to finalize the protocol for apoptosis assessment. In order to achieve consistent protein expression (approximately 60%) across samples, we performed a multitude of transfection assays to adjust the amount of DNA plasmids added to each sample. Next, we checked the protein expression in transfected cells every 12 hours until the percentage of cells expressing viral proteins has reached our desired level. This was done to ensure that the cells were allowed to grow and express the protein for Geneticin (G418, an analog of neomycin sulfate) resistance under non-selective conditions prior to antibiotic selection. Additionally, we carried out multiple trials of G418 selection to optimize the concentration of G418 and the length of selection since the cells can develop resistance to the antibiotic if insufficient concentration is used or if selected for a long period of time. We also passaged the cells every 2 days after the selection started to prevent overgrowth of untransfected cells that have yet to be selected by G418. Lastly, we used 2% sodium dodecyl sulfate (SDS) to solubilize the dye taken up by the cells and measured optical density at 590 nm using a spectrophotometer to quantify cell viability from the crystal violet staining experiment.

Here we described the protocol developed to quantitatively assess the apoptotic activity of the viral proteins in cancer cells, as shown in Fig. 1. Specifically, the p53-null non-small cell lung carcinoma H1299 cells were transiently transfected with EGFP-tagged constructs. Two days post-transfection, the percentage of cells expressing viral constructs (regardless of the relative amount) was assessed using fluorescence microscopy. The construct expression was visualized by the presence and distribution of EGFP fluorescence across cells in each sample. Following the confirmation of protein expression, H1299 transfected cells were selected using G418 to ensure that only EGFP-positive cells remain for the analysis of apoptotic activity. The cells were maintained in increasingly concentrated G418 medium for 4 days or until the cells in the negative selection controls were completely removed by G418. Crystal violet staining was then performed to assess apoptotic activity of each sample. The dye taken up by the cells was then solubilized by SDS and the optical density was measured spectrophotometrically at 590 nm to give direct measures of cell viability.

As expected, treatment of the no transfection sample with G418 medium resulted in an empty well with no viable cells, while the no transfection sample treated with G418-free medium remained populated with viable cells (Fig. 4a). The data indicate that construct-negative cells were effectively removed from samples treated with G418, leaving only transfected cells.

Once we established a method that would allow for a clear interpretation of apoptotic activity, we transfected H1299 cells with the following EGFP-tagged constructs: PCV1 VP3 N-terminal homologous region (EGFP – PCV1 VP3, 1-105 aa), PCV1 VP3 C-terminal extended region (EGFP – PCV1 VP3, 105-207 aa), and EGFP – CAV VP3 – PCV1 VP3 C- terminal extended region chimera (EGFP – CAV VP3, 1-121 aa, – PCV1 VP3, 105-207 aa) (Fig. 2). To establish positive apoptosis controls, H1299 cells were transfected with untruncated EGFP-

tagged proteins including wt CAV VP3 (EGFP – wt CAV VP3, 1-121 aa) and wt PCV1 VP3 (EGFP – wt PCV1 VP3, 1-207 aa) (Fig. 2). Negative apoptosis controls included an empty EGFP vector and a no transfection sample.

Following transfection, we assessed the percentage of cells expressing the constructs by visualizing the distribution of EGFP expression. As depicted in Fig. 3a, the distribution of EGFP fluorescence was consistent across the tested samples (approximately 60%), meaning that the percentage of construct-positive cells was relatively uniform. Quantification of the distribution of EGFP expression across cells using ImageJ, however, failed to recapitulate the visual evaluation of the samples under the microscope, as shown in Fig. 3b. Interestingly, wt CAV VP3 and PCV1 VP3 N-terminal homologous region exhibited bright fluorescence while wt PCV1 VP3, PCV1 VP3 C-terminal extended region, and the chimeric viral protein fluoresced dimly. Additionally, visual assessment of the transfectants revealed that wt CAV VP3 not only localized in the nucleus but also exhibited punctate localization patterns, while the N-terminal region of PCV1 VP3 displayed a diffuse localization throughout the cell similar to the EGFP control vector, as shown in Fig. 3a. The wt PCV1 VP3, C-terminal region of PCV1 VP3, and the chimeric viral protein localized in the cytoplasm and shared similar semi-punctate localization patterns. The noticeable variation in EGFP intensity and localization between the constructs containing the C-terminal region and the ones lacking it may suggest that the C-terminal region of PCV1 VP3 is responsible for these differences. The presence of the extended region may drive the overall conformation of wt PCV1 VP3 and the chimeric protein, resulting in structures displaying dim fluorescence and semi-punctate localization pattern.

Following the confirmation of protein expression, H1299 cells were treated with G418 for selection of construct-positive cells and then stained with crystal violet for detection of viable cells (Fig. 4a). Among the EGFP-tagged constructs, cell viability was statistically significant (*P<0.05; **P<0.02; ***P<0.001; n=3) when compared with the control EGFP vector (Student's t- test), as shown in Fig. 4b. The expression of wt PCV1 VP3 resulted in an almost complete loss of H1299 cells similar to the no transfection sample treated with G418 (1% and 0% viability, respectively) (Fig. 4). This result indicates that wt PCV1 VP3 possesses a very robust apoptotic activity. Surprisingly, wt CAV VP3 had no appreciable apoptotic activity as indicated by a higher viability compared to the control EGFP vector (21% vs. 12% viability, respectively). Interestingly, previous studies have shown that FLAG – wt CAV VP3, a polypeptide protein-tagged version of the construct, possesses powerful apoptosis induction (40). These data indicate that the fusion of EGFP to the N-terminal end of wt CAV VP3 remarkably hinders its apoptotic activity.

The truncation mutagenesis studies also show that the C-terminal extended region induced more apoptosis than the N-terminal homologous region (6% vs. 24% viability, respectively) (Fig. 4). Surprisingly, the transfection of H1299 cells with CAV VP3 – PCV1 VP3 C-terminal extended region chimera resulted in an increased apoptosis level when compared with the transfection of wt CAV VP3 (7% vs. 21% viability, respectively). These results indicate that the C-terminal extended region of PCV1 VP3 mutant not only operates independently of the N-terminal homologous region, but also rescues a nonfunctional protein and still maintains a strong apoptotic activity comparable to wt PCV1 VP3. Additionally, it is possible that the apoptotic activity of the N-terminal region of PCV1 VP3 is inhibited by the N-terminal fusion of EGFP, similar to the case of EGFP – wt CAV VP3.

DISCUSSION

Current anticancer therapies are limited by their toxicity to normal tissue and dependence on functional p53 tumor suppressor protein. Since about half of all human cancers have mutations in p53, there is an urgent need for a treatment that can selectively target cancer cells regardless of their p53 status. It has been shown that several members of the *Circoviridae* family encode proteins that can induce apoptosis in p53-null cancer cell lines. Chicken anemia virus (CAV), the most characterized members of its family, possesses a third viral protein (VP3) with demonstrated apoptotic activity. Interestingly, CAV VP3 only induces apoptosis in cancer cells, and not in normal cells. Another virus originating from the same family, Porcine Circovirus Type 1 (PCV1), has also been shown to possess a VP3 with functional similarity to CAV VP3. However, very little is known about PCV1 VP3. Recent sequence analysis of the protein revealed an N-terminal region homologous to CAV VP3 and a C-terminal extended region. This study aimed to continue previous efforts to determine how efficiently PCV1 VP3 induces apoptosis in cancer cell and to identify the genomic region responsible for the apoptosis-inducing property.

Our apoptosis studies show that wt PCV1 VP3 possesses a very robust apoptotic activity. While the N-terminal region of PCV1 VP3 was expected to be responsible for this powerful characteristic due to its high sequence homology shared with the potent apoptosis inducer, CAV VP3, it appeared to be non-functional when truncated from the C-terminal region. Surprisingly, the C-terminal region of PCV1 VP3 was found to be essential for apoptosis induction, causing cell death with similar strength and morphologic features as the untruncated protein. This finding is particularly intriguing since neither of the homologues of PCV1 VP3 possess a C-terminal extended region, suggesting that PCV1 VP3 causes cell death via a mechanism that is expected

to differ from CAV VP3 and PCV2a/b. This hypothesis is reinforced by the analysis of localization patterns and cell cycle arrest data from previous studies [9, 10]. Specifically, it has been shown that CAV VP3 induces G2/M cell cycle arrest and localizes in the nucleus of cancer cells and in the cytoplasm of normal cells, while PCV1 VP3 induces G1 cell cycle arrest and localizes in the cytoplasm of both transformed and primary cells. These results taken together with the findings of our truncation mutagenesis experiments give us reason to envision the possibility that PCV1 VP3 induces apoptosis using an alternative pathway. If our current interpretation of the results holds true, we envision future studies that continue truncation mutagenesis experiments to isolate the specific sequence that triggers programmed cell death of PCV1 VP3.

The role of the N-terminal homologous region of PCV1 VP3 still remains largely unknown. Our data show that the N-terminal region did not result in any appreciable apoptosis compared to the full-length protein and was morphologically indistinguishable from an empty EGFP vector control. Additionally, the apoptotic ability of the C-terminal region was comparable to the full-length protein but slightly diminished. Together, these data indicate that the N-terminal region may have a role in enhancing the apoptotic ability of the C-terminal region. For instance, this may be achieved if the addition of N-terminal region creates a different tertiary structure which causes wt PCV1 VP3 to be slightly more apoptotic than the C-terminal region alone. Alternatively, we suspect that the N-terminal region of PCV1 VP3 may harbor its own role in apoptosis induction. However, its ability may have been lost due to truncation. The loss of its apoptotic capacity may be attributed to its potential need for interaction with the C-terminal region, for example, in order to achieve proper folding. We foresee that uncoupling the exact role of the N-terminal region will rely on having clear evidence discerning whether the N-terminal

and the C-terminal regions of PCV1 VP3 are, in fact, different domains and therefore, form independent tertiary structures.

Regardless of how the two regions of PCV1 VP3 interact with each other, the lack of apoptotic activity observed in the N-terminal region may also be explained by the potentially hindering fusion of EGFP to its N-terminus. This speculation arises from noticing a similar deleterious effect in the N-terminally EGFP-tagged wt CAV VP3 construct. If this explanation turns out to be correct, it may also imply that the robust apoptotic activity observed in EGFP – wt PCV1 VP3 may not be representative of its full potential. This means that in the absence of EGFP fusion, wt PCV1 VP3 may be capable of causing even more drastic cell death than the fused version of wt PCV1 VP3 with EGFP. Based on these speculations, we suggest creating and testing constructs from the *Circoviridae* family that are either C-terminally EGFP-tagged or that do not utilize a fluorescent tag at all, in which case a FLAG-tag could be used.

It is important to note that although our study shows strong evidence that the fusion of EGFP to the N-terminus of wt CAV VP3 ablates its ability to induce apoptosis, its distinct punctate pattern of aggregation and preferential localization in the nucleus of cancer cells remains unchanged (data not shown). This unexpected finding suggests that the localization behavior of CAV VP3 may not be directly related to its apoptotic ability. Previous studies have shown that interaction of CAV VP3 with the APC1 subunit of the anaphase-promoting complex/cyclosome (APC/C) results in apoptosis in cancer cells [21]. Furthermore, CAV VP3 mutants that maintain nuclear localization but do not interact with the APC1 subunit of the APC/C, fail to induce apoptosis in cancer cells [9]. Our data are consistent with these findings and we envision that the N-terminal fusion of EGFP may alter the APC1 binding site of CAV

VP3, preventing the association of the APC1 subunit with the protein. This may explain why EGFP – wt CAV VP3 failed to induce apoptosis, but still localized in the nucleus of cancer cells.

While studies have shown that FLAG-tagged wt PCV1 VP3 and CAV VP3 both selectively induce apoptosis in cancer cells and not in normal cells, the EGFP-tagged constructs including truncated mutants have not been tested. Since the ability of the protein to discriminate between cancer cells and normal cells is of outmost importance to cancer treatment, it is necessary to verify that its cytotoxicity is unique to transformed cells and does not affect primary cells.

FIGURES

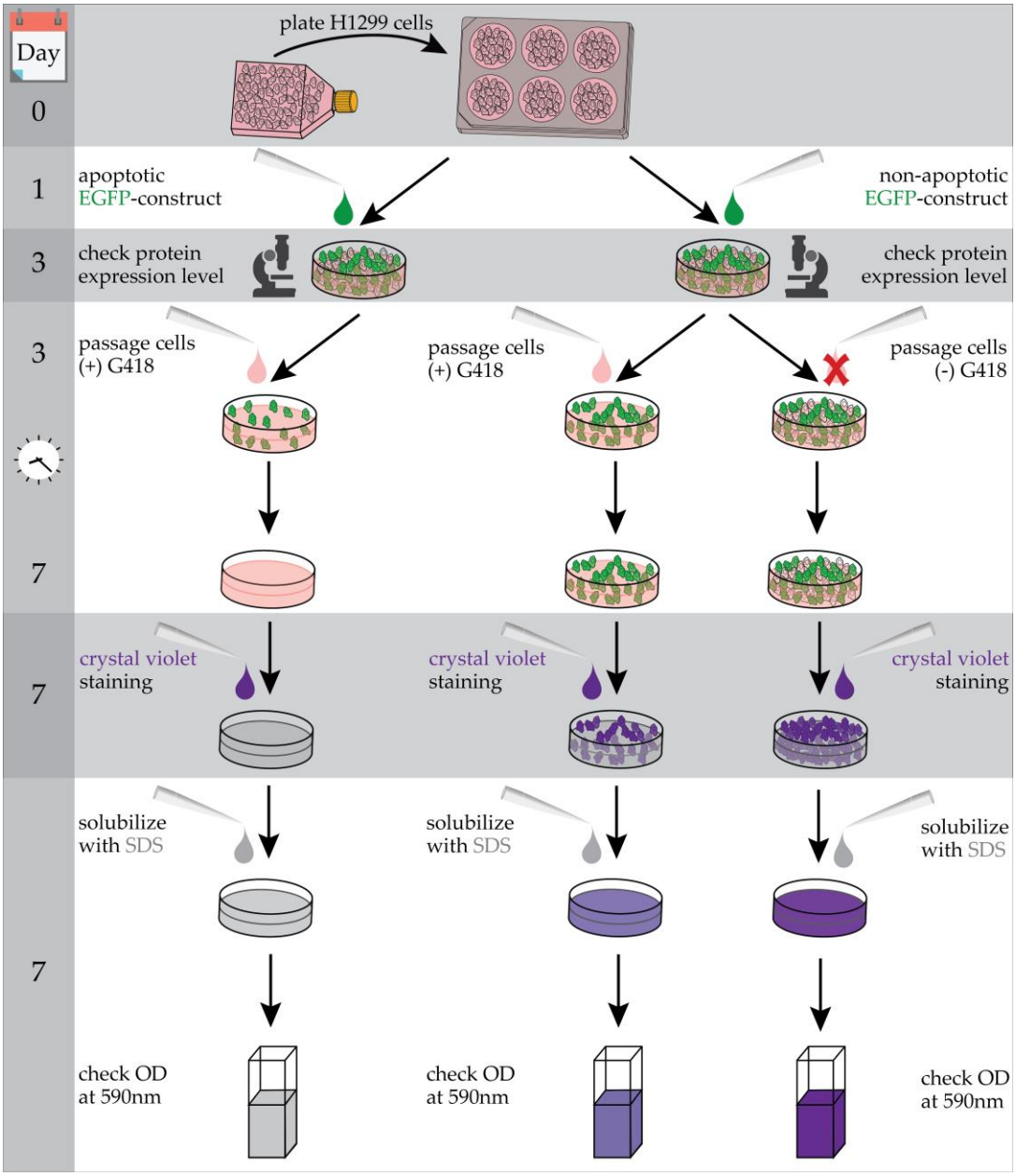

FIG. 1. Experimental timeline. (Day 0) H1299 cells were passaged into 6-well plates. (Day 1) Confluent cells were transiently transfected with N-terminal EGFP-tagged constructs. (Day 3) Transfected cells were visualized by fluorescence microscopy for EGFP expression. H1299 cells were then passaged at 7:10 dilution and selected with G418 [0.8 mg/ml] for construct-positive cells. (Day 5) Cells were passaged again and further selected with G418 [1.2 mg/ml]. (Day 7) G418 selected H1299 cells were stained with crystal violet to visualize cell viability, with darker staining representing more viable cells. Constructs with apoptotic ability were expected to result in an empty well with no viable cells, while constructs with no apoptotic ability were expected to result in a populated well with viable cells. To quantify cell viability, crystal violet taken up by cells was solubilized with SDS and optical density (OD) was measured spectrophotometrically at 590nm.

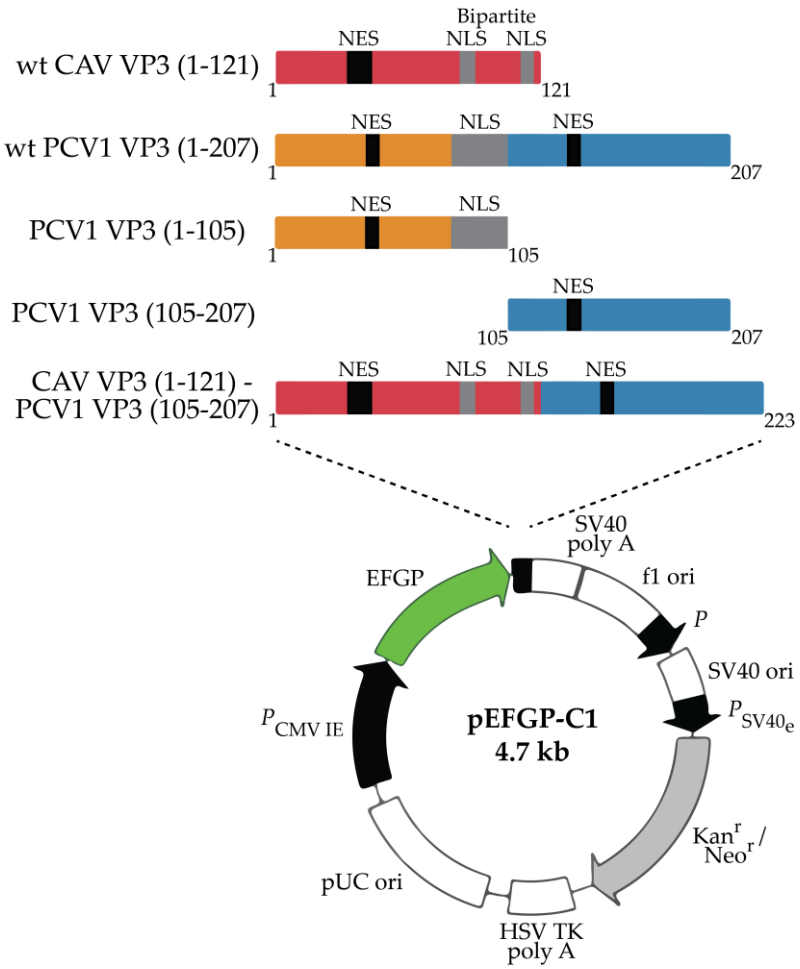

FIG. 2. Schematic diagram of N-terminal EGFP-tagged constructs. The genes of interest were cloned into pEGFP-C1 vector under the control of a constitutive cytomegalovirus (CMV) promoter to make the following recombinant constructs: EGFP – wt CAV VP3 (1-121 aa), EGFP – wt PCV1 VP3 (1-207 aa), EGFP – PCV1 VP3 N-terminal homologous region (1-105 aa), EGFP – PCV1 VP3 C-terminal extended region (105-207 aa), and EGFP – CAV VP3 – PCV1 VP3 C-terminal extended region chimera (1-223 aa).

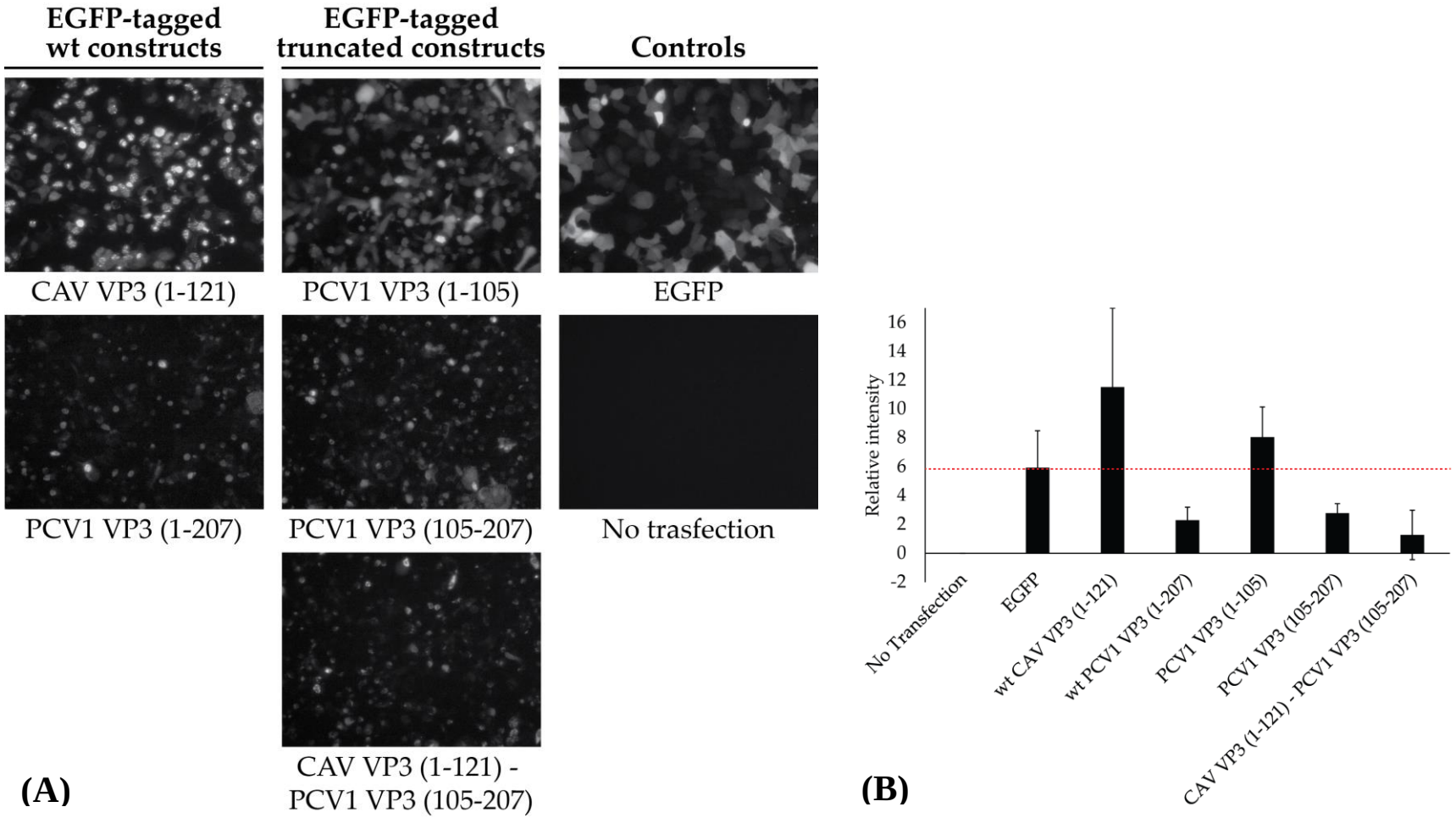

FIG. 3. Variation in levels of EGFP expression among recombinant constructs. (A) H1299 cells were transiently transfected in 6-well plates with EGFP-tagged constructs. Transfected cells were imaged 2 days post-transfection with a Zeiss Vert.A1 inverted fluorescence microscope using SPOT 5.1 Basic software. Shown samples are representative of three independent experiments. To improve contrast between green and black pixels, images were converted to a greyscale. (B) The EGFP expression of transfected H1299 cells in each panel was calculated by white pixel intensity using ImageJ, normalized to the no transfection sample, and shown as mean ± SD. Student's t-test showed no significant difference between expression levels when compared with an empty vector, here denoted as EGFP (n=3).

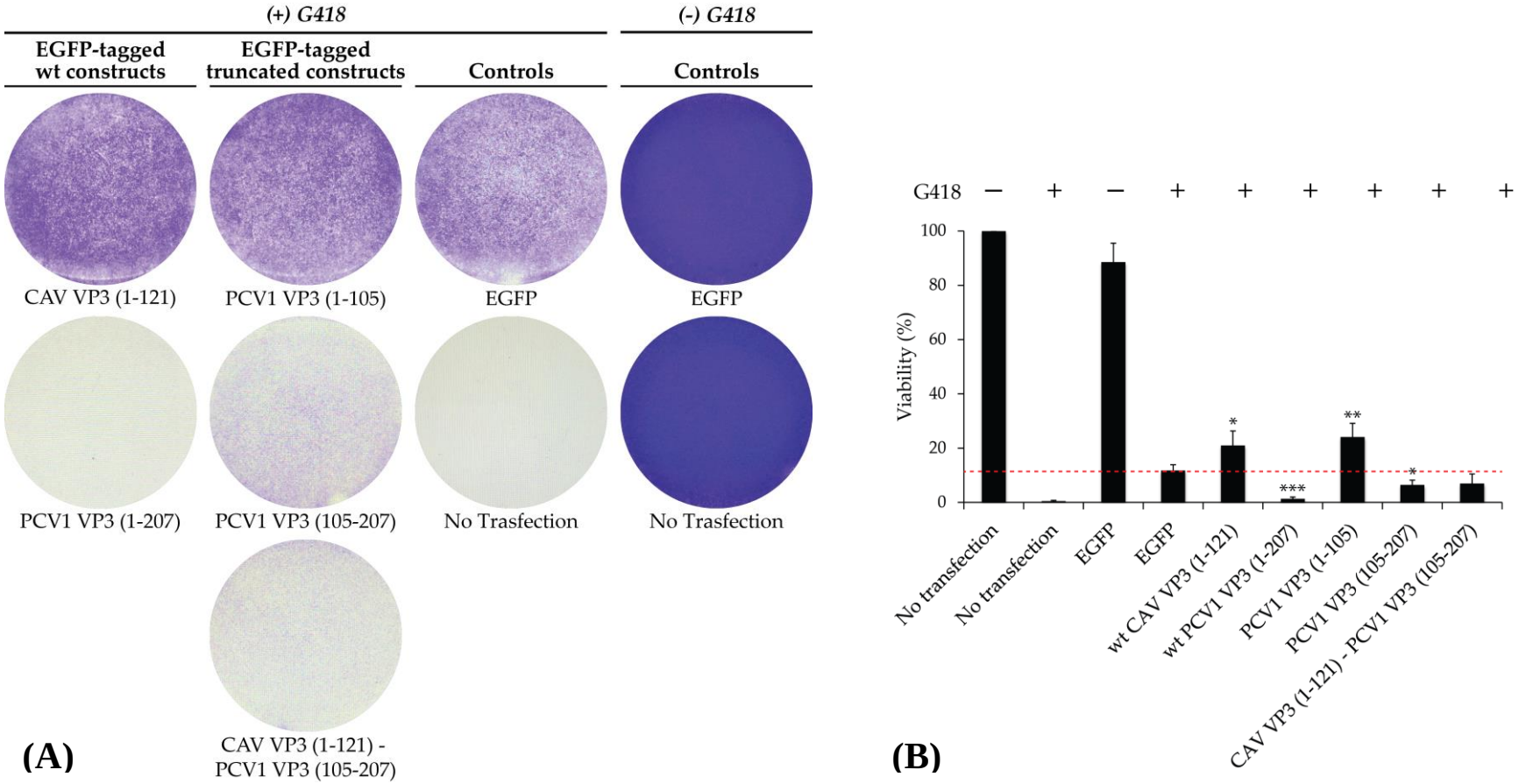

FIG. 4. Crystal violet staining of H1299 cells after transfection and G418 selection revealed the importance of the C-terminal extended region of PCV1 VP3 in inducing apoptosis. (A) H1299 cells were transiently transfected in 6-well plates with EGFP-expression constructs. H1299 cells were then treated with increasing amount of G418 [0.8 mg/ml - 1.2 mg/ml] 2 days post-transfection (+ G418). Two G418 selection controls (empty EGFP vector and no transfection) were treated with G418-free medium (- G418). H1299 cells were selected for 4 days, fixed, and stained with crystal violet, with darker staining representing more viable cells. Shown samples are representative of three independent experiments. (B) Following crystal violet staining, SDS was used to solubilize the dye and the percentage of viable H1299 cells was calculated based on optical density measured at 590nm. Data were normalized to the no transfection sample treated with G418-free medium and shown as mean ± SD. *P<0.05; **P<0.02; ***P<0.001 when compared with an empty vector, here denoted as EGFP with G418-containing medium; n=3 (Student's t-test).

REFERENCES

1. Danen-Van Oorschot, A.A., D.F. Fischer, J.M. Grimbergen, B. Klein, S. Zhuang, J.H. Falkenburg, C. Backendorf, P.H. Quax, A.J. Van der Eb, and M.H. Noteborn, *Apoptin induces apoptosis in human transformed and malignant cells but not in normal cells.* Proc. Natl. Acad. Sci. USA, 1997. **94**(11): p. 5843-7.
2. Danen-Van Oorschot, A.A., A.J. van der Eb, and M.H. Noteborn, *BCL-2 stimulates Apoptin-induced apoptosis.* Adv. Exp. Med. Biol., 1999. **457**: p. 245-9.
3. Edwards, B.K., A.M. Noone, A.B. Mariotto, E.P. Simard, F.P. Boscoe, S.J. Henley, A. Jemal, H. Cho, R.N. Anderson, and B.A. Kohler, *Annual Report to the Nation on the status of cancer, 1975-2010, featuring prevalence of comorbidity and impact on survival among persons with lung, colorectal, breast, or prostate cancer.* Cancer, 2014. **120**(9): p. 1290-1314.
4. Gagnon, C.A., D. Tremblay, P. Tijssen, M.H. Venne, A. Houde, and S.M. Elahi, *The emergence of porcine circovirus 2b genotype (PCV-2b) in swine in Canada.* Can. Vet. J., 2007. **48**(8): p. 811-9.
5. Guimaraes, D.P. and P. Hainaut, *TP53: a key gene in human cancer.* Biochimie, 2002. **84**(1): p. 83-93.
6. Hamel, A.L., L.L. Lin, and G.P. Nayar, *Nucleotide sequence of porcine circovirus associated with postweaning multisystemic wasting syndrome in pigs.* J. Virol., 1998. **72**(6): p. 5262-7.
7. Hanahan, D. and R.A. Weinberg, *The Hallmarks of Cancer.* Cell, 2000. **100**(1): p. 57-70.
8. Heilman, D.W., M.R. Green, and J.G. Teodoro, *The anaphase promoting complex: a critical target for viral proteins and anti-cancer drugs.* Cell Cycle, 2005. **4**(4): p. 560-3.
9. Heilman, D.W., J.G. Teodoro, and M.R. Green, *Apoptin nucleocytoplasmic shuttling is required for cell type-specific localization, apoptosis, and recruitment of the anaphase-promoting complex/cyclosome to PML bodies.* J. Virol., 2006. **80**(15): p. 7535-45.
10. Hough, K.P., A.M. Rogers, M. Zelic, M. Paris, and D.W. Heilman, *Transformed cell-specific induction of apoptosis by porcine circovirus type 1 viral protein 3.* Journal of General Virology, 2015. **96**(Pt 2): p. 351-359.
11. Jeurissen, S.H., F. Wagenaar, J.M. Pol, A.J. van der Eb, and M.H. Noteborn, *Chicken anemia virus causes apoptosis of thymocytes after in vivo infection and of cell lines after in vitro infection.* J. Virol., 1992. **66**(12): p. 7383-8.
12. Kiupel, M., G.W. Stevenson, E.J. Galbreath, A. North, H. HogenEsch, and S.K. Mittal, *Porcine circovirus type 2 (PCV2) causes apoptosis in experimentally inoculated BALB/c mice.* BMC veterinary research, 2005. **1**(1): p. 7.
13. Liu, J., I. Chen, and J. Kwang, *Characterization of a previously unidentified viral protein in porcine circovirus type 2-infected cells and its role in virus-induced apoptosis.* Journal of Virology, 2005. **79**(13): p. 8262-8274.

14. Meehan, B.M., F. McNeilly, D. Todd, S. Kennedy, V.A. Jewhurst, J.A. Ellis, L.E. Hassard, E.G. Clark, D.M. Haines, and G.M. Allan, *Characterization of novel circovirus DNAs associated with wasting syndromes in pigs.* J. Gen. Virol., 1998. **79 (Pt 9)**: p. 2171-9.
15. O'Connor, C., J.U. Adams, and J. Fairman, *Essentials of Cell Biology.* NPG Education, Cambridge, 2010.
16. Peters, J.M., *The anaphase-promoting complex: proteolysis in mitosis and beyond.* Mol. Cell, 2002. **9**(5): p. 931-43.
17. Rogers, A.M. and K.P. Hough, *The Effect of Subcellular Localization on the Oncoapoptotic Capability of Porcine Circovirus Type 1 VP3*, in *Department of Chemistry and Biochemistry*. 2012, B.S. Thesis. Worcester Polytechnic Institute: Worcester, MA.
18. Roulston, A., R.C. Marcellus, and P.E. Branton, *Viruses and apoptosis.* Annu. Rev. Microbiol., 1999. **53**: p. 577-628.
19. Segales, J. and M. Domingo, *Postweaning multisystemic wasting syndrome (PMWS) in pigs. A review.* Vet. Q., 2002. **24**(3): p. 109-24.
20. Sherr, C.J., *Principles of tumor suppression.* Cell, 2004. **116**(2): p. 235-46.
21. Teodoro, J.G., D.W. Heilman, A.E. Parker, and M.R. Green, *The viral protein Apoptin associates with the anaphase-promoting complex to induce G2/M arrest and apoptosis in the absence of p53.* Genes Dev., 2004. **18**(16): p. 1952-7.
22. Thornberry, N.A. and Y. Lazebnik, *Caspases: enemies within.* Science, 1998. **281**(5381): p. 1312-1316.
23. Tischer, I., R. Rasch, and G. Tochtermann, *Characterization of papovavirus-and picornavirus-like particles in permanent pig kidney cell lines.* Zentralbl Bakteriol Orig. A, 1974. **226**(2): p. 153-67.
24. Todd, D., *Circoviruses: immunosuppressive threats to avian species: a review.* Avian Pathol., 2000. **29**(5): p. 373-94.
25. Zhuang, S.M., A. Shvarts, H. van Ormondt, A.G. Jochemsen, A.J. van der Eb, and M.H. Noteborn, *Apoptin, a protein derived from chicken anemia virus, induces p53-independent apoptosis in human osteosarcoma cells.* Cancer Res., 1995. **55**(3): p. 486-9.